Parallel-field electrorheological clutch: Enhanced high shear rate performance

Liyu Liu, Xixiang Huang, and Cai Shen
Department of Physics and Institute of Nano Science and Technology, The Hong Kong University of Science and Technology, Clear Water Bay, Kowloon, Hong Kong, China

Zhengyou Liu and Jing Shi
Department of Physics, Wuhan University, Wuhan, China

Weijia Wen[a] and Ping Sheng
Department of Physics and Institute of Nano Science and Technology The Hong Kong University of Science and Technology, Clear Water Bay, Kowloon, Hong Kong, China

(Received 27 May 2005; accepted 1 August 2005; published online 2 September 2005)

We present an electrorheological (ER) fluid cylindrical clutch which achieves stable shear stress at high shear rate, and demonstrates superior performance compared with the traditional ER clutches. The design is realized by employing alternate-stripe electrodes on the inner cylinder, with either dielectric or metallic outer rotor. The alternate stripe electrodes generate electric fields with a component parallel to the shearing direction, so that ER particles can form chain structures parallel to shear and thereby bring significant enhanced device performance at a high shear rate. Differences due to the use of dielectric or metallic outer rotor are shown to be compatible with expectations based on simulated electric-field patterns. © *2005 American Institute of Physics*.
[DOI: 10.1063/1.2042535]

Electrorheological (ER) fluid is a colloidal suspension consisting of micro- or nanosized particles. Its apparent viscosity can be tunable through the externally applied electric-field strength.[1–5] Such a unique field-induced property is very useful for many potential applications in industry and engineering, such as clutch and damping systems.[6,7] However, all of these devices require high mechanical performances of ER fluid under relatively high electric field.[8] For some dynamic devices, the clutch for example, the shear rate dependence of the ER effect is a critical issue. It is well known that in all two-plate ER fluid clutches, a generic problem is the loss of ER functionality at high shear rates.[9] It is generally observed that the shear stress increases initially as a function of shear rate upon the application of the electric field, reaching a maximum below 10 s^{-1} and then decreases significantly.[10] One reason for this behavior is purely geometric: The ER shear strength always follows the electric-field direction, along the axis of chains or columns formed with ER particles as illustrated in Fig. 1 (upper left panel). Upon shearing, the chains/columns will lean in the direction of the shear with an angle θ with respect to the applied field direction $\mathbf{E}_0$, and the strength of the chains/columns is thereby decreased by a geometric factor $\cos\theta$ (upper right panel). Since angle θ increases with increasing shear rate, partial loss of ER functionality results. Another reason is that once the chains break at high shear rate, the segments cannot form stabilized chains again because of ER particles separation/expulsion under the centrifugal force. On the lower panel of Fig. 1, we show the measured results of a parallel-plate ER clutch, in which the ER fluid used is the same as those used in the tests described below. The decline in shear stress is clearly seen at higher shear rates.

In order to overcome the problems described above, we present a new design employing the so-called parallel electrode configuration, where the electric field can have a component *parallel* to the shearing direction of the chains or columns. In that case, regardless of the shear rate, there will always be a significant projection of the line of force on the (imaginary) line joining the particles, thus offering greater resistance to shear and thereby retaining the ER functionality

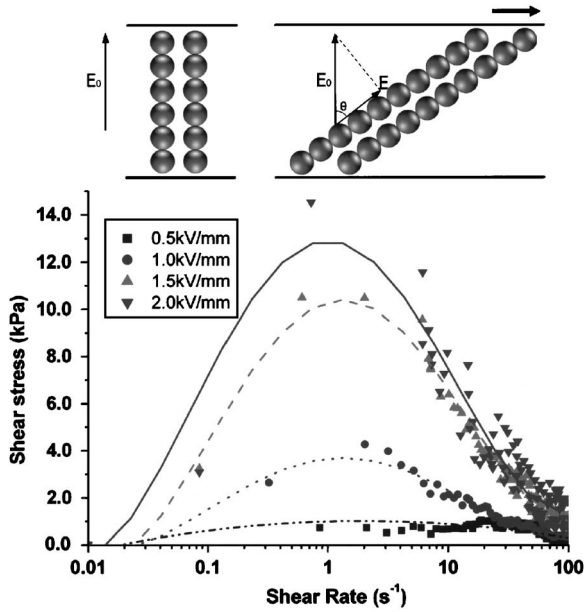

FIG. 1. Schematic illustration of the of ER particle chains under an electric field with no shear (upper left panel) and with shear (upper right panel). Since the line of force is along the electric-field direction, the right panel shows the chains are weakened when they lean at an angle θ with respect to the field direction. In the lower panel, measured data for a parallel-plate ER clutch are shown. The ER fluid used is similar to those used in tests shown in Fig. 2.

[a]Author to whom correspondence should be addressed; electronic mail: phwen@ust.hk

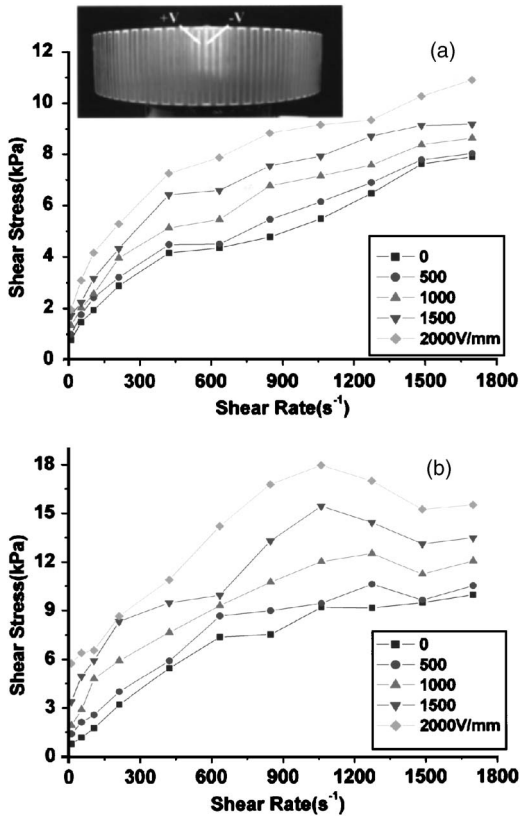

FIG. 2. Performance of the parallel-field clutch under different applied voltages, plotted versus shear rate. The upper inset in (a) shows the structures of the stripe electrodes employed on the surface of the clutch's inner cylinder, with plus and minus voltages applied alternately. In (a), the outer rotor is made of Teflon, and the shear stress of the clutch is seen to increase monotonically with shear rate and voltage. In (b), the outer rotor is made of aluminum, and a peak in the shear stress is seen.

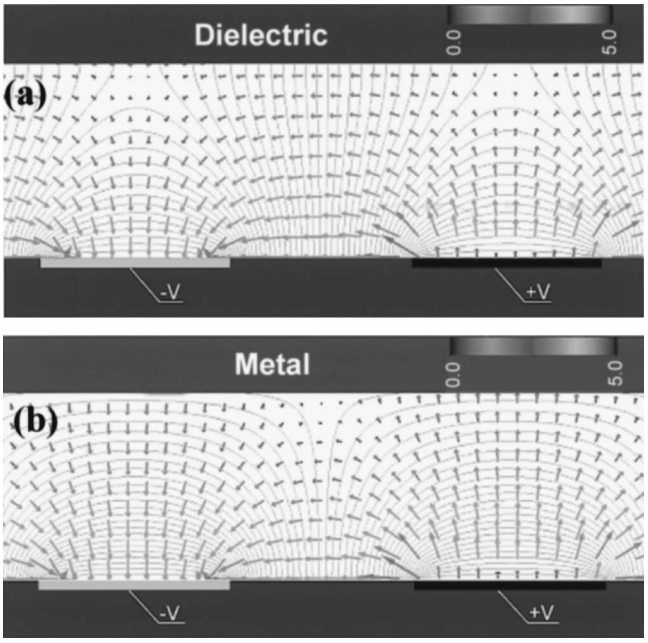

FIG. 3. Calculated electric fields with dielectric (a) and conducting (b) upper boundaries. In (a), the electric field is seen to be predominantly parallel to the two surfaces, and the perpendicular component is relatively small. But in (b), the metallic boundary condition at the upper surface means that, except close to the lower surface, the field component is predominantly perpendicular to the two surfaces. The overall field intensity is higher in (b) due to the fact that metallic boundary condition completely confines the electric field to the gap region.

even under high shear rates. Our experimental results verify this expectation.

The ER fluid used in the experiments is synthesized as follows. Polymethylmethacrylate (PMMA) microspheres were modified by coating them with polyethylenimine (PEI), an effective dispersent in aqueous solution. The PEI-coated microspheres form the "seeds" in solutions of oxalic acid, with barium chloride, rubidium chloride, and titanium tetrachloride added in the ratio as $Ba_{0.9}Rb_{0.1}TiO(C_2O_4)_2$. Urea was subsequently added slowly. The reaction was performed in an ultrasonic bath at 65 °C. After the reaction, a thin layer of barium titanyl oxalate nanoparticles with rubidium doping and urea coating (BTRU for short) was formed on the surface of the modified PMMA microspheres due to the oppositely charged BTRU nanoparticles and the (PEI-coated) PMMA surface. The resulting powder is mixed with silicone oil in the composition of 5 grams of solid powder to 10 ml of oil, to form a colloid and injected into the clutch that has the parallel field design, described below.

The parallel-field ER clutch consists of a cylindrical outer rotor and a concentric cylindrical inner stator on which a cup-shaped stripe electrodes are mounted, such that the perpendicular stripes, extending from the top to bottom of the inner stator, alternate along the circular surface of the stator and form the + and − electrodes. The alternating positive and negative voltages applied along the stator surface are illustrated in the upper inset of Fig. 2(a), where the separation between the perpendicular stripes is 1 mm, and the gap between the inner and outer cylinder (inner surface) is 1 mm. The outer rotor is made of either insulating (Teflon) or conducting material (aluminum) for the purpose of altering the electric-field configuration in the gap region, so as to facilitate testing the parallel-field premise.

It is well known from electrostatics that if the separation between the stripes is ℓ, then significant electric field will extend outward from the cylindrical surface to a distance $\sim\ell$. Moreover, the electric field will have a significant component which is parallel to both the surface of the cylinder, and perpendicular to the stripes. In the present design, there is a gap between the circular surface of the rotor and the outer cylinder, wherein ER fluid is disposed. The gap has to be on the order of ℓ, so that there is significant electric field filling the entire gap. When relative rotation is imposed between the inner and outer cylinders, it can be seen that the shearing distortion would be parallel to some component of the electric field.

The measured ER effect versus shear rate is shown in Fig. 2(a) for the clutch that has the outer rotor made of insulating dielectric Teflon. We can see that, unlike the traditional two-plate clutches whose shear stress starts to decrease at shear rate >10 s^{-1}, the shear stress of the present clutch increases with increasing shear rate up to 1800 s^{-1}, reaching 11 kPa at 2 kV/mm. This result confirms our theoretical expectation stated before, and offers a solution to the generic problem in ER fluid applications. Figure 2(b) shows the measured results for the clutch that has the outer rotor made of aluminum. Since the conducting boundary changes the electric-field pattern inside the gap region, different clutch performance is expected. From Fig. 2(b), it is seen that the maximum shear stress can reach 18 kPa at shear rate of 1100 s^{-1}, stronger than that with insulating outer rotor case.

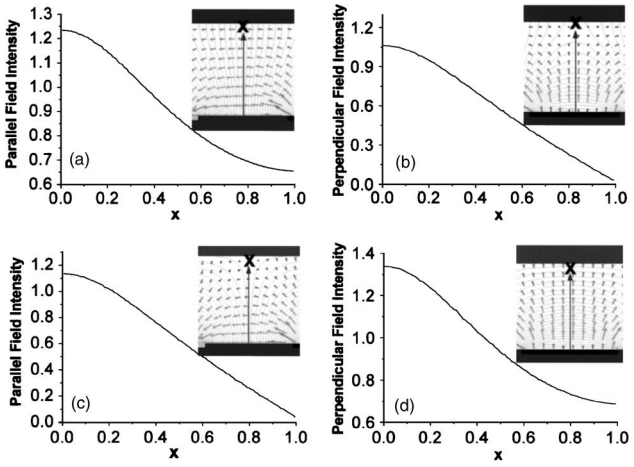

FIG. 4. Parallel and perpendicular electric-field intensities for outer rotors made with dielectric material [(a) and (b)] and metallic material [(c) and (d)]. In (a) and (c), the parallel component of the field intensity is plotted as a function of distance along the line situated at the midpoint between the two electrodes. In (b) and (d), the perpendicular component of the field intensity is plotted as a function of distance along the line situated at the midpoint of one of the electrodes. Here, zero distance is defined to be the surface of the inner rotor (stator), and 1 denotes the inner surface of the outer rotor.

However, the shear stress exhibits a gentle decline when the shear rate is beyond 1100 s^{-1} before it stabilizes.

To explain our experimental observations, we numerically solve the Laplace equation by the finite element method and calculate electric-field distributions for the different cases of two different outer cylinders. Figures 3(a) and 3(b) show the field distributions with insulating and conducting boundary conditions, respectively. The parameters used are the same as those in the experiment. The dielectric constant value of 2 was used for Teflon in the simulation, whereas a perfect conducting boundary condition was used in the metallic case. In the figures, arrows are used to delineate the field distribution, with length of the arrows and colors provide information about the field intensity: The stronger the field, the longer the arrow. It is seen that there is a more parallel component of the electric field in the case of dielectric outer rotor, but due to the fact that there is leakage of the electric field into and beyond the outer rotor, the overall electric-field intensity in the gap region is somewhat lower than the case of the metallic outer rotor, which completely confines the electric field inside the gap region, but which also induces a more perpendicular component of the electric field.

In Figs. 4(a) and 4(b) plot the calculated parallel and perpendicular components of the electric field for the case of dielectric outer rotor. In Fig. 4(a), the field intensity parallel to the direction of shearing, along the indicated red line (perpendicular to the midpoint between two electrodes), is plotted as a function of distance from the inner rotor surface. The result shows that the parallel-field intensity close to the lower plate is stronger than that at the outer rotor, with an approximate linear variation in between. The field at the outer rotor surface is about 0.65 (in arbitrary units), or ~50% of that at the inner rotor surface, which presents the largest resistance to shear. In Fig. 4(b), the field component perpendicular to the shearing direction is similarly plotted along a line perpendicular to the midpoint of one of the electrodes. It is seen that the field intensity drops linearly from 1.05 at the inner rotor surface to almost 0 at the outer rotor surface. Since parallel fields occupy a majority of the gap space in this case, the clutch thus exhibits an outstanding performance at high shear rates, with monotonically increasing shear stress as a function of shear rates [see Fig. 2(a)]. A different situation is seen when the dielectric outer rotor is replaced by a conducting outer rotor, as can be seen in Figs. 4(c) and 4(d). For the conducting outer boundary, the parallel component of the field intensity [Fig. 4(a)] drops from about 1.1 at the inner stator surface to zero at the outer rotor surface as required by the metallic boundary condition, while the perpendicular component of the field intensity decreases by about 50% from 1.35 units to 0.7 at the midpoint of one of the electrodes [Fig. 4(d)]. Therefore, it is clear that in the case of the conducting outer rotor, the field component in the gap region is mostly perpendicular to the shearing direction. As the performance of the clutch mostly depends on the perpendicular field at low shear rates, ER particle chains formed under the perpendicular field would thus be able to provide better shear resistance, leading to the observed higher shear stress. But with increasing shear rates, our geometric argument predicts a drop in shear stress, which was indeed observed [Fig. 2(b)]. With still a further increase in shear rates, the conducting outer rotor case exhibits a stabilized shear stress, owing to the existence of the parallel-field component, mostly in the region close to the inner stator surface.

From the results presented above, it is seen that the advantage(s) of our design at high shear rates can be further enhanced by using a high-dielectric constant material for the outer rotor (so as to prevent leakage of the electric field), and by decreasing the gap to about one-half of the spacing between the electrodes.

The authors would like to acknowledge the support of grants from the NSFC/RGC (No. N HKUST605/04) and Hong Kong RGC (No. 604104).

[1] M. Whittle and W. A. Bullough, Nature (London) **358**, 373 (1992).
[2] Y. Chen, A. F. Sprecher, and H. Conrad, J. Appl. Phys. **70**, 6796 (1991).
[3] H. J. Choi, M. S. Cho, J. W. Kim, C. A. Kim, and M. S. Jhon, Appl. Phys. Lett. **78**, 3806 (2001).
[4] W. J. Wen, X. Huang, S. Yang, K. Lu, and P. Sheng, Nat. Mater. **2**, 727 (2003).
[5] X. Pan and G. H. McKinley, Appl. Phys. Lett. **71**, 333 (1997).
[6] A. E. Smith and L. F. Evans, Proc. SPIE **66**, 5051 (2003).
[7] A. R. Johnson, W. A Bullough, and J. Makin, Smart Mater. Struct. **8**, 591 (1999).
[8] S. K. Chung and H. B. Shin, IEEE Trans. Veh. Technol. **53** (2004).
[9] Y. Tian, Y. Meng, H. Mao, and S. Wen, Phys. Rev. E **65**, 031507 (2002).
[10] W. Wen, X. Huang, and P. Sheng, Appl. Phys. Lett. **85**, 299 (2004).